Precipitation behavior of Ag–Pd–In dental alloys

Y. C. SUH, Z. H. LEE
Department of Materials Science and Engineering, Korea Advanced Institute of Science and Technology, 373-1 Kusung-Dong, Yusung-Gu, Taejon, 305-701, South Korea
E-mail: s_syc@cais.kaist.ac.kr, zhlee@kaist.ac.kr

M. OHTA
Department of Dental Materials Engineering, Faculty of Dentistry, Kyushu University, 3-1-1 Maedashi, Higashi-ku, Fukuoka 812-82, Japan
E-mail: ohtadeh@mbox.nc.kyushu-u.ac.jp

Age-hardening characteristics and precipitation behavior of Ag–25%Pd–3%In–1%Zn–0.5%Ir alloy were investigated in detail by means of hardness testing, X-ray diffraction, electron microscopy and resistivity measurement. The solution treating could be accomplished at 980 °C and the aging in the temperature range from 950 to 850 °C occurred by continuous precipitation. The aging in the temperature range from 850 to 450 °C occurred first, forming GP-zones with a hardness increase and then in overaging stage by forming discontinuous precipitation, which consisted of lamellae of solute (Pd, In, Zn) depleted Ag-rich phase and $(Pd,Ag)_3(In,Zn)$ intermetallic phase. The hardness increased very fast to its peak in 10 min during aging at temperatures between 450 and 550 °C.

1. Introduction

The high price of gold dental alloys has created a demand for cheaper crown and bridge alloys, which have been met by manufacturers to the extent that a variety of alternative alloys are now available. These alternative alloys fall into three main categories: gold-reduced alloys, silver–palladium alloys and base metal alloys. The silver–palladium alloys have recently been used widely because of their low cost, reasonably good castability and corrosion resisting properties. Another favorable feature of this type of alloy is its age-hardenability when the elements such as Cu, Zn, Sn, Ga and In are added [1]. It is well known that Cu is the principal hardener and Sn, Ga, and In have a smaller effect on hardening. A small amount of Zn is added for deoxidizing the melt and improving casting fluidity [2].

The precipitation behavior of Ag–Pd–Cu alloys has been investigated in several studies [3–5]. The results of their experiments can be summarized as follows. The age hardening of Ag–Pd–Cu alloys occurred in two stages: spinodal decomposition of the homogeneous matrix into a modulated coherent structure (stage I), and the discontinuous precipitation of a CuPd ordered phase and a Ag-rich phase from the supersaturated solid solution (stage II). Usually, the discontinuous precipitation cells initiate at grain boundaries and advance into the grain interiors, resulting in lamellar aggregates of equilibrium α and γ phases behind an advancing interface. This precipitation is characterized by discontinuous changes in orientation and composition across the migrating interface between the two matrix phases α and α', which is the reaction front, providing a short circuit path of solute transport [6].

The Ag–Pd–In base alloy is being newly developed as a dental alloy and there seems to be no publication reporting the precipitation behavior of this alloy. Therefore it is the purpose of this paper to study comprehensively the precipitation and age hardening behavior of a dental Ag–Pd–In alloy.

2. Experimental procedure

The nominal chemical composition of the alloy used was Ag–25%Pd–3%In–1%Zn–0.5%Ir as shown in Table I. A small amount of Zn and Ir were added for deoxidizing the melt and improving casting fluidity, and for grain refining, respectively. The alloy melt was prepared from pure metals of a purity better than 99.99% in a vacuum induction melting furnace and then cast in a graphite mold. As the total weight loss in the melting process was less than 0.02%, chemical analysis after melting was not carried out. The ingots were cold-worked slightly and homogenized at 980 °C for 2 h and then cut into pieces of $5 \times 5 \times 3$ mm size for hardness tests and the metallographic observations. The homogenized specimens were also rolled to plates of about 0.1 mm and 0.18 mm thickness for the transmission electron microscopic studies and the resistivity measurements, respectively.

The aging behavior was examined by hardness tests, X-ray diffraction (XRD), resistivity measurements, scanning electron microscopy (SEM) and transmission electron microscopy (TEM). Hardness tests were performed with a 25 g (and) or 200 g load using a micro-Vickers' hardness tester. The load of 25 g was used to measure the hardness of the small lamellae area

TABLE I Chemical composition of Ag–25%Pd–3%In–1%Zn–0.5%Ir alloy

Alloys	Ag	Pd	In	Zn	Ir
wt %	70.5	25	3	1	0.5
at %	70.1	25.2	2.8	1.6	0.3

alone. The hardness values were averages of ten indentations. Area fractions of the lamellae were measured from microphotographs (× 150). X-ray diffraction study was performed in a RINT-2500V standard-type diffractometer (Rigaku Co. Ltd) to identify the phases formed during the discontinuous precipitation. The X-ray source was a rotating anode copper target operating at 40 kV and 200 mA. CuK_α radiation was used as the incident beam. Powder specimens prepared by a grinding method [7] were vacuum sealed in a silica tube and subjected to heat treatment at the required temperatures and period. The parametric method [8] was used to determine the solvus line and lattice parameters were determined by the least-square method. Electrical resistivity was measured during continuous heating in vacuum from room temperature to 900 °C at a constant rate of 0.1 °C min^{-1} by the four-terminal potentiometric method with a direct current of 200 mA. The specimens for microstructure examination were etched in a solution of 2.5% KCN and 2.5% $(NH_4)S_2O_8$ in water and examined in a Phillips scanning electron microscope. Specimens for TEM were thinned using a double-jet technique. The electrolyte used was a mixture of perchloric acid, glycerin and ethanol. SEM and TEM observations were made with P-515 and CM200 microscopes operating at 30 kV and 200 kV, respectively. In addition, the liquidus and solidus temperatures of the alloy were measured with quenched specimens in a differential thermal analyzer (Rigaku Co. Ltd) during continuous heating and cooling between room temperature and 1400 °C at a constant rate of 5 °C min^{-1}.

3. Results and discussions

3.1. Solution treatment temperature

Fig. 1 shows a part of the typical DTA curve obtained by heating and cooling the specimen. The exothermic peak of cooling curve and the endothermic peak of the heating curve were observed at the temperatures of 1051 and 1157 °C, respectively. Fig. 2 shows the SEM micrographs of the alloy annealed at 980 and 950 °C for 1 h. A second phase was observed in Fig. 2b but not in Fig. 2a. On this basis, the solution treatment temperature of 980 °C was chosen to produce the supersaturated solid solution. The solution treated specimen showed a XRD pattern of the α_0 single phase of the face centered cubic structure, as will be shown in Fig. 8.

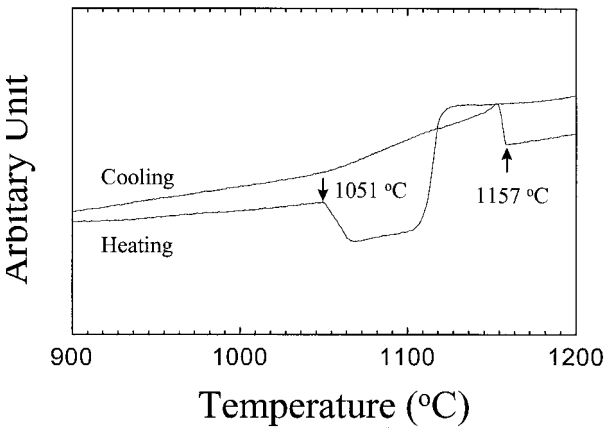

Figure 1 A typical DTA curve of Ag-25%Pd-3%In-1%Zn-0.5%Ir alloy.

3.2. Aging behavior

Fig. 3 shows aging behavior of the solution-treated and quenched specimen examined by heating excursion of electrical resistivity measurement (ERM). The curve (a) demonstrates the relative resistivity based on the room temperature value. The resistivity increases with temperature and starts to decrease at around 380 °C and reaches a minimum value at about 560 °C and then rises again. The curve (b) shows the temperature derivative of the curve (a). The resistivity decrease at around 350 °C is due to the start of the precipitation, and the peak at 560 °C suggests that the most of the precipitation has already taken place, and the resistivity increases again due to the thermal vibration.

Fig. 4 shows the variation of hardness during isothermal aging at constant temperatures. These aging temperatures were determined from the ERM result. A supersaturated solid solution exhibited remarkable hardening during aging. The hardness curves showed generally the expected behavior of age hardening. The precipitation of this Ag–Pd–In alloy is controlled by

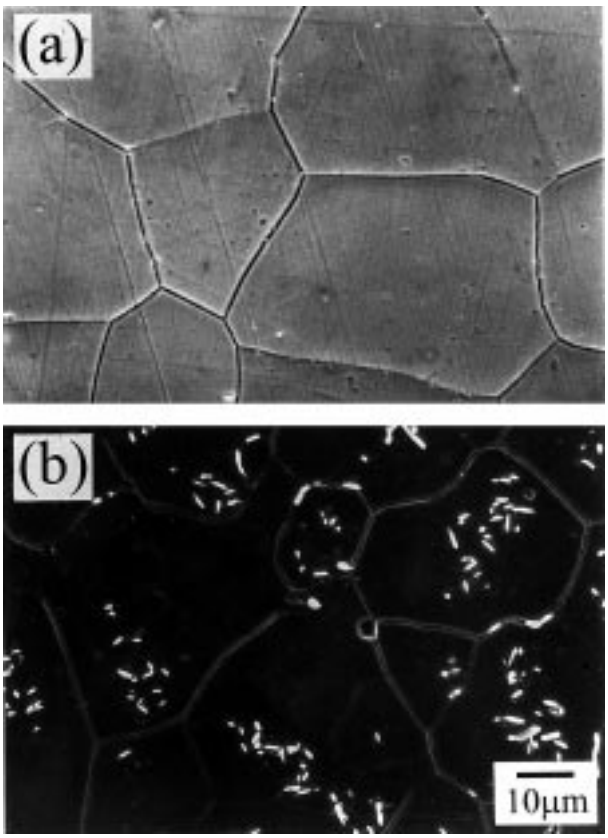

Figure 2 SEM micrographs of Ag-25%Pd-3%In-1%Zn-0.5%Ir alloy annealed at (a) 980 °C and (b) 950 °C for 1 h and then quenched into ice-brined.

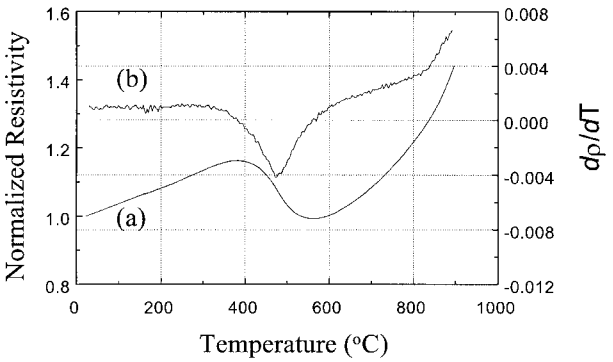

Figure 3 Changes in (a) the electrical resistivity and (b) its temperature derivative.

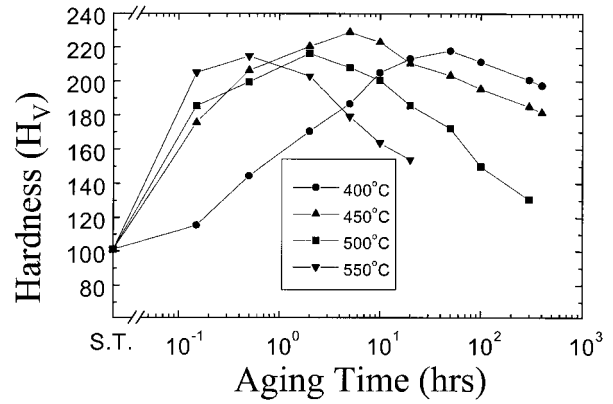

Figure 4 Variation of hardness during isothermal aging at constant temperature. The test was made at a load of 200 g.

diffusion mechanism and the hardening rate is much slower than that of Ag–Pd–Cu alloys, which hardens by spinodal decomposition and discontinuous precipitation [9].

Figs 5 and 6 show SEM and TEM micrographs of this alloy after solution treating at 980 °C and aging for 1 h at various temperatures. On aging at 450 °C, some fine particles were precipitated along grain boundaries in the initial stages of aging (Figs 5d and 6d). With increasing aging time, such particles grew from grain boundaries into grain interior, resulting in lamellar structure (Fig. 6c). With increasing aging temperature, the lamellar structure developed faster (Figs 5c and 6b). Fig. 5c shows that the lamellar structure covers the whole grains. In general, it is possible to form the lamellar structure by two kinds of transformation modes; eutectoid reaction and discontinuous precipitation. The discontinuous precipitation is characterized by discontinuous changes in orientation and composition between the matrix phase across the migrating interface, the reaction front, which provides a short circuit path of solute diffusion. There is no change in the crystal structure between the super-saturated matrix and the depleted matrix, and this characteristic distinguishes discontinuous precipitation from the morphologically similar eutectoid reaction [6].

3.3. Discontinuous precipitation

In order to determine the composition of each phase, microanalysis was carried out at a resolution of less than 10 nm by the energy-dispersive-X-ray spectroscopy (EDS) of transmission electron microscopy (TEM).

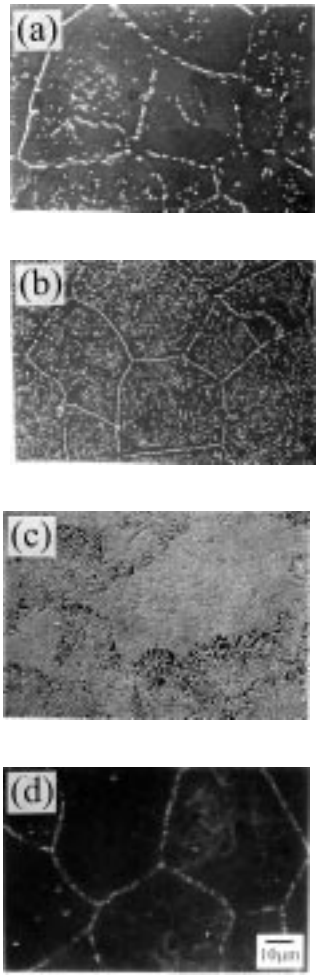

Figure 5 SEM micrographs after aging at various temperatures for one hour; (a) 930 °C, (b) 850 °C, (c) 650 °C and (d) 450 °C.

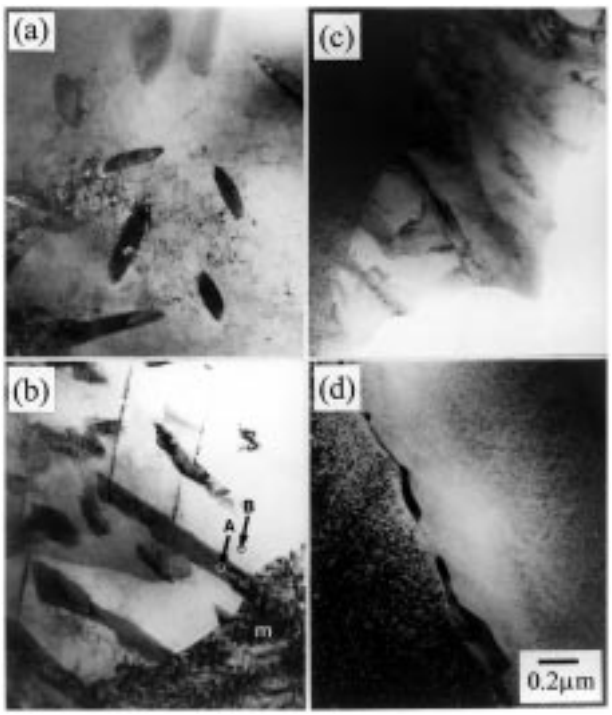

Figure 6 TEM bright-field images after aging at (a) 850 °C for 1 h, (b) 550 °C for 1 h, (c) 450 °C for 30 h and 450 °C for 30 h.

Table II presents the result of this analysis taken from the area marked by arrows in Fig. 6b. It was impossible to analyze a small amount of iridium component. The α_0

TABLE II The EDS microanalysis of Ag–25%Pd–3%In–1%Zn–0.5%Ir alloy at the region marked in Fig. 6b

Region		Ag	Pd	In	Zn
A-region	wt %	23.2	57.2	13.6	5.9
	at %	22.4	55.9	12.3	9.4
B-region	wt %	74.5	23.1	1.7	0.8
	at %	69.4	23.2	1.6	1.3
m-region	wt %	65.7	27.6	5.2	1.5
	at %	65.0	27.7	4.8	2.5

matrix (m-region) had a composition close to the average composition of the alloy. The A-region was a newly precipitated Pd-rich phase close to the composition of $(Pd,Ag)_3(In,Zn)$, and the B-region had a somewhat higher Ag content compared to the α_0 matrix. It can be considered that the A-region and the B-region indicate a γ precipitate and a solute-depleted α matrix respectively. Indium atoms go predominantly into palladium intermetallic phase.

Another important feature of the discontinuous precipitation is characterized by discontinuous changes in orientation between the matrix phase across the migrating interface. Fig. 7 shows TEM micrographs of the alloy aged at 550 °C for 1 h. Fig. 7a shows a bright-field image of lamellar aggregates. Fig. 7b shows the selected area diffraction pattern (SADP) taken from matrix (M-region) marked by arrow in Fig. 7a using the smallest size of aperture. This indicates the matrix has face-centered cubic structure with [0 1 1] zone axis. Without changing tilt angle, the SADP of high zone axis taken from solute-depleted phase (B-region) marked by an arrow in Fig. 7a was obtained as shown in Fig. 7c. By comparing Fig. 7b with 7c, it is clear that M-region and B-region have the same f.c.c. structure but are different in orientation. From the results of Table II and Fig. 7, it can be concluded the lamellar structure develops from grain boundaries by discontinuous precipitation.

On the other hand, separate plate-like precipitates were formed by aging above 850 °C (Figs 5a, b and 6a). Above 850 °C, the amount of precipitates decreased with increasing temperature. It can be considered that the continuous precipitation is predominant over the discontinuous precipitation in this high temperature, and the lamellar structure develops in the lower temperature range of 450–840 °C.

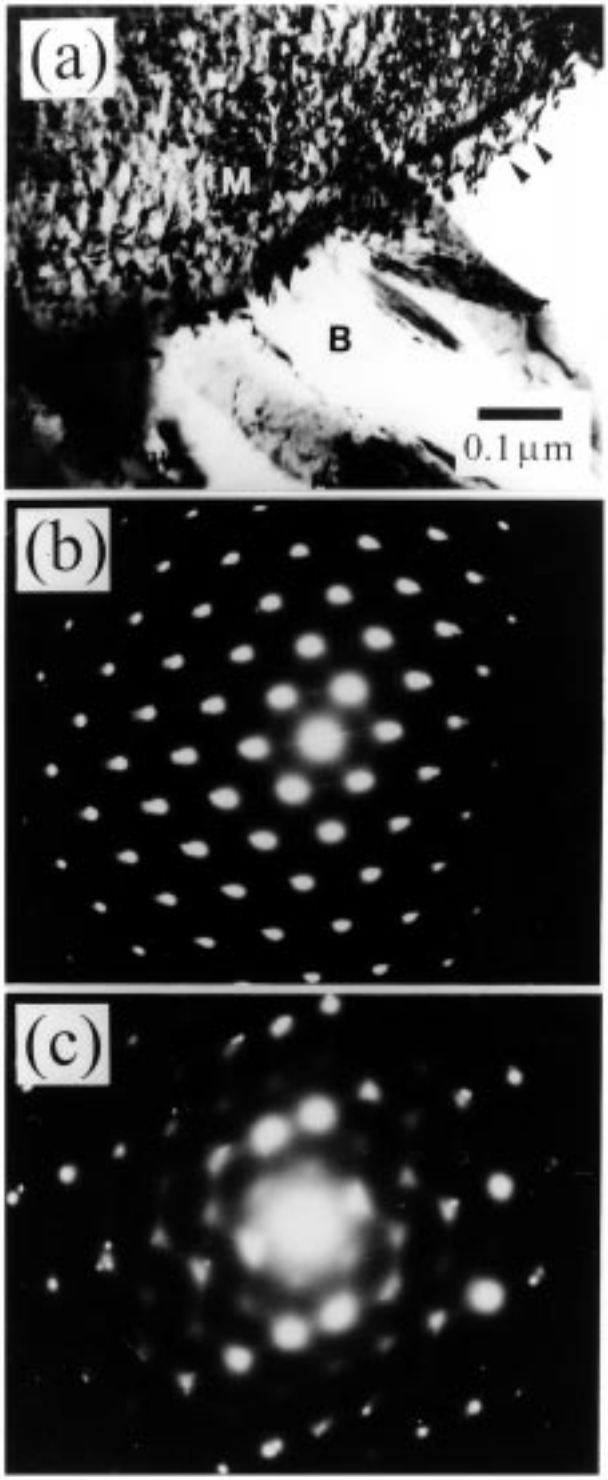

Figure 7 TEM micrograph of AG-25%Od-3%In-1%Zn-0.5%Ir alloys after solution treating at 980 °C for 1 h, quenching and aging at 550 °C for 1 h; (a) bright-field image, (b) diffraction pattern of [011] zones axis taken from M region market in Fig. 7a, (c) diffraction pattern of higher zone axis taken from B region marked in Fig. 7a.

3.4. XRD spectrum of discontinuous precipitates

In order to identify the phases of lamellar product observed in Figs 5 and 6, XRD patterns were taken from the powder specimens aged for various lengths of time. Fig. 8 presents the changes in the XRD pattern during isothermal aging at 550 °C. The solution-treated specimen gave an XRD pattern of the α_0 single phase of the face centered cubic (f.c.c.) structure with lattice parameter $a = 0.40349$ nm. The intensities of the diffraction peak of the precipitates increased with increasing aging time. This precipitate (γ) has been identified as $(Pd,Ag)_3(In,Zn)$ (Al_3Ti type) with a c/a ratio of about 1.22. This value is different from that of Pd_3In in the binary Pd–In system which is 0.90 $\sim$ 0.93 [10]. That is, the lattice parameter of the γ phase in the Ag–Pd–In system is elongated more toward the c axis. This is probably due to higher silver content in the γ phase.

The XRD profiles of Fig. 8 also show that the diffraction peak of the supersaturated α_0 phase decreased in peak width with the formation of stable $(Pd,Ag)_3(In,Zn)$ precipitate. This may be related to precipitation such as clustering or GP zone which gives rise to diffuse scattering around the positions of the fundamental Bragg peaks. Theoretical consideration of

diffuse X-ray scattering suggests that the formation of GP zone or spinodal decomposition does not cause a shift in the position of the fundamental Bragg reflection [11]. Consequently, the measurements of the lattice parameter during the decomposition of a supersaturated solid solution can provide a method of distinguishing preprecipitation from precipitation. The lattice parameter of the matrix did not change during aging time between 0.5 and 3 h, as shown in Fig. 8. The hardening during initial stage of aging is caused by the clustering and GP zone. However, the preprecipitation could not be clarified because a spot image of the matrix with progress of the aging was not examined by TEM analysis in this study.

Fig. 9 shows the area fraction of lamellar product formed by aging at 550 and 650 °C for various periods. The area fraction increases with increasing aging time and aging temperature. This fact means that the diffraction pattern of the specimen aged at 550 °C for 10 h in Fig. 8 is attributed to the formation of lamellar product. There were, however no diffraction peaks of Ag-rich matrix of lamellar product in Fig. 8. It can be considered that as the difference of lattice parameter between α_0 matrix and α Ag-rich matrix is very small, the diffraction peaks will be overlapped in the XRD pattern. As is evident with Figs 6 through 9 and Table II, we can conclude that the lamellar products formed at grain boundaries consist of Ag-rich matrix and $(Pd,Ag)_3(In,Zn)$ precipitates.

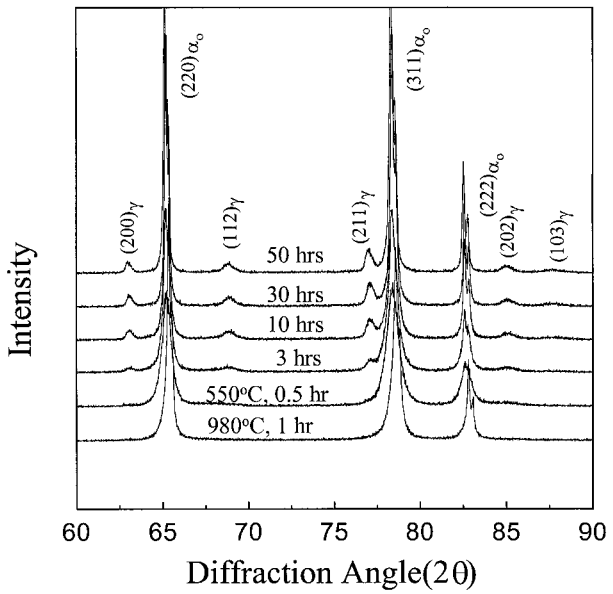

Figure 8 The diffractograms of Ag-25%Pd-3%In-1%Zn-0.5%Ir alloys after solution treated at 980 °C for 1 h and aged at 550 °C for 0.5, 3, 10, 30, and 100 h.

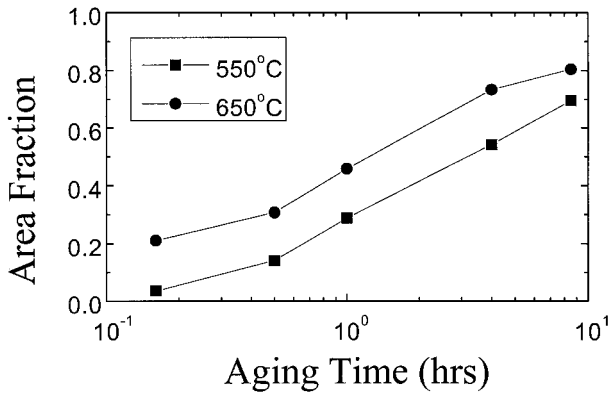

Figure 9 Variation of area fraction of lamellar product formed in Ag-25%Pd-3%In-1%Zn-0.5%Ir alloys as a function of aging times.

3.5. The aging behavior at elevated temperature

Figs 10 and 11 show the hardness change of the alloy aged at various temperatures at which the discontinuous precipitation is dominant. The age hardening curves in Fig. 10 were measured with a 200 g load and the indent covered the grain interior and the lamellar product

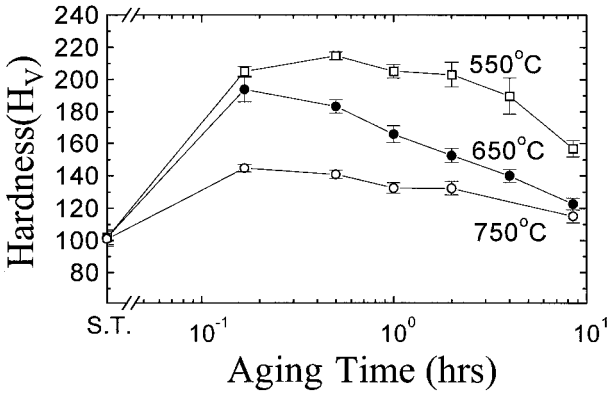

Figure 10 Variation of hardness of Ag-25%Pd-3%In-1%Zn-0.5%Ir alloys as a function of aging times. The test was made at a load of 200 g.

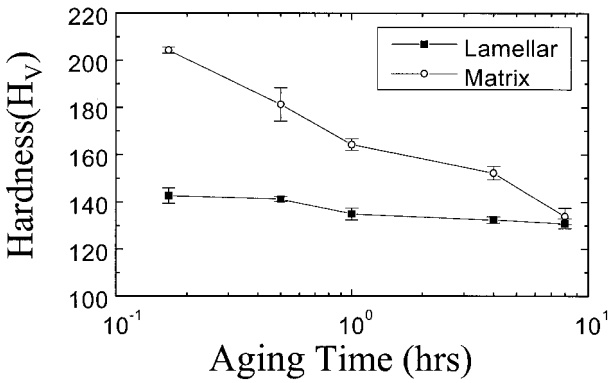

Figure 11 Variation of hardness in the grain interior and the lamellar product aged at 650 °C as a function of aging time. The test was made at a load of 25 g.

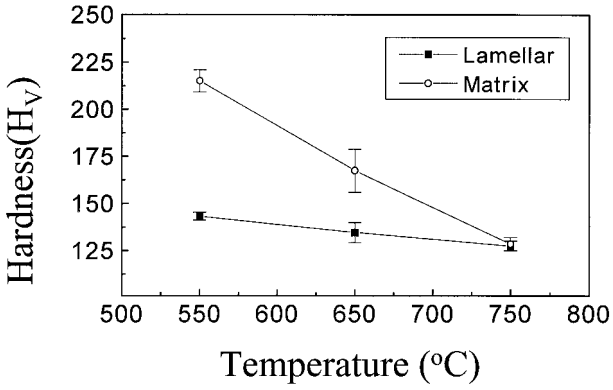

Figure 12 Variation of hardness in the grain interior and the lamellar product aged at various temperatures for 1 h. The test was made at a load of 25 g.

together. The hardness increases from the initial value of 101 VHN to the maximum of 215 VHN in 10 min at 550 °C and then decreases gradually with aging time. This decrease is attributed to the formation and the growth of lamellar structure. The hardness in the grain interior and the lamellar product was separately measured with small weight of 25 g load, as shown in Fig. 11. The hardness in the grain interior decreased with increasing aging time, while the hardness in the lamellar product was not changed. Fig. 12 shows that the temperature dependence of hardness is larger in the grain interior than in the lamellar product. This indicates that the hardening at elevated temperature is caused by the precipitation of a particular phase in the grain interior, and the lamellar formation corresponds to overaging.

Fig. 13 shows the reaction-front of the discontinuous precipitation in the alloy aged at 650 °C for 10 h, which advances into the grain where coarsened γ precipitates formed by continuous precipitation already exist. The crystallographic structure of the continuous precipitates can be considered to correspond to that of the discontinuous γ precipitates from the results of Figs 8 and 9. The discontinuous reaction is an effective way of rapid coarsening of the continuous precipitates and lowering the free energy [6], and can be expressed in the form of

$$\alpha_0 + \gamma \rightarrow \alpha + \gamma$$

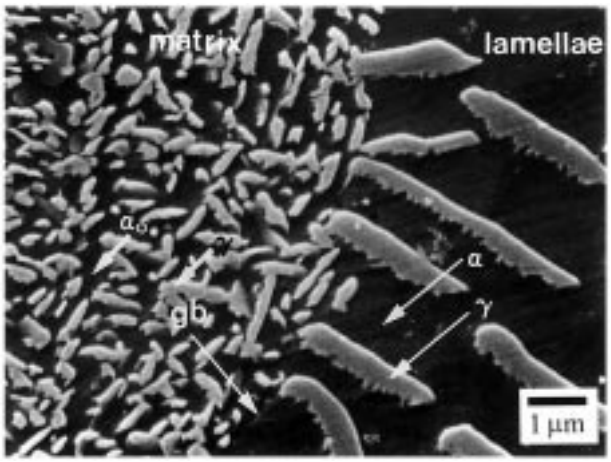

Figure 13 SEM micrograph of the aloy aged 650 °C for 10 h. The lamellae are grouwing from the right to the left consuming the grain consisting of supersaturated α_o solid solution and γ precipiates forming lamellae γ and α solid sulution close to the equilibrium composition.

4. Conclusions

Age-hardening characteristics and discontinuous precipitation of Ag–Pd–In alloys were investigated by means of hardness testing, X-ray diffraction, electron microscopy and resistivity measurement. The following results were obtained.

1. A discontinuous precipitation reaction at grain boundaries in Ag–Pd–In alloys has occurred by aging in the temperature range 450–840 °C. Above 850 °C the precipitation occurred continuously.

2. A lamellar structure developed by discontinuous reaction consisted of Ag-rich matrix and $(Pd,Ag)_3(In,Zn)$.

3. The decrease in hardness of the specimen in the overaging stage at elevated temperature was attributed first to the coarsening of γ preprecipitates in the matrix and then to the formation of lamellae by discontinuous precipitation.

4. The discontinuous reaction at temperatures at which the discontinuous precipitation is dominant was expressed in the form of $\alpha_0 + \gamma \rightarrow \alpha + \gamma$.

Acknowledgments

The research was performed under a financial support from KOSEF and Myoungbo Dental Company under grant number 96-2-06-04-01-3. The authors wish to thank Dr Shiraishi, Dr Machuya and Dr Nakagawa of Kyushu University and Mr Uhm of Myoungbo Dental Company for helpful discussions.

References

1. R. M. GERMAN, *Int. Met. Rev.* **27** (1982) 260.
2. R. M. GERMAN, M. M. GUZOWSKI and D. C. WRIGHT, *J. Metals* **32** (1980) 20.
3. M. M. KARNOWSKY, *J. Mater. Sci.* **13** (1978) 2339.
4. M. OHTA, K. HISATSUNE and M. YAMANE, *J. Less-Common Metals* **65** (1979) 11.
5. I. KAWASIMA, Y. KANZAWA, Y. ARAKI and H. OHNO, *J. Jpn Inst. Metals* **53** (1989) 14.
6. D. B. WILLIAMS and E. P. BUTLER, *Int. Met. Rev.* **26** (1981) 153.
7. Y. C. SUH, Z. H. LEE and M. OHTA, *J. Mater. Sci. Lett.* 1998, in prep.
8. B. D. CULLITY, ''Elements of X-ray diffraction'' 2nd edn (Addison-Wesley, Wokingham 1978) p. 360.
9. I. KAWASHIMA, Y. ARAKI and H. OHNO, *J. Mater. Sci.* **26** (1991) 1113.
10. S. BHAN and K. SCHUBERT, *J. Less-Common Metals* **17** (1969) 73.
11. A. KRAWITZ and R. SINCLAIR, *Phil. Mag.* **31** (1975) 697.

Received 3 April
and accepted 31 August 1998